Dear Editor-in-Chief,

We take this opportunity to thank you, and Referee 1 for thoughtful comments on our manuscript which helped us in improving the manuscript. We hope that the answer of each major and minor comment will meet your expectations. The comments of the reviewers and their replies are listed here one by one, which includes some figure also.

Yours sincerely,

Rahul Prajapati, Kusumita Arora

Major Problems:

Comment 1. The authors applied two methods to measure the fractal dimensions. They should simply describe the methods and clearly explain the parameters. For example, the authors should explain the definitions of 'length' and 'k' in Figure 1.

Answer 1. We have revised the methodological section and incorporated the sentences and equations which describe the methods and clearly explain the parameters involved in both the methods. The revisions also include the definition of 'length' and 'k' used in Figure 1. The revised section of methodology is attached at the end of all comments and answers (Page 10-14). The methodological section of manuscript has also revised accordingly.

Comment 2. The authors must use a testing example to describe the way applied to estimate the values of multifractal spectrum, i.e., h_w, and to explain whether or not the estimated values are reliable. This will help me to accept the results.

Answer 2: For the testing example, we have taken the 128 data samples of vertical component of geomagnetic field on 13 May, 2019 and 01:00:00 to 01:02:08 hrs. (Figure 1 f) to explain the way multifractal spectrum values (hw) is estimated. The estimation of multifractal spectrum using wavelet leader technique comprises of following four steps:

(i) In the first step we applied the discrete wavelet transform and decomposed the signal at five levels and restored the values of detail and approximation wavelet coefficients (Figure 1 a-f).

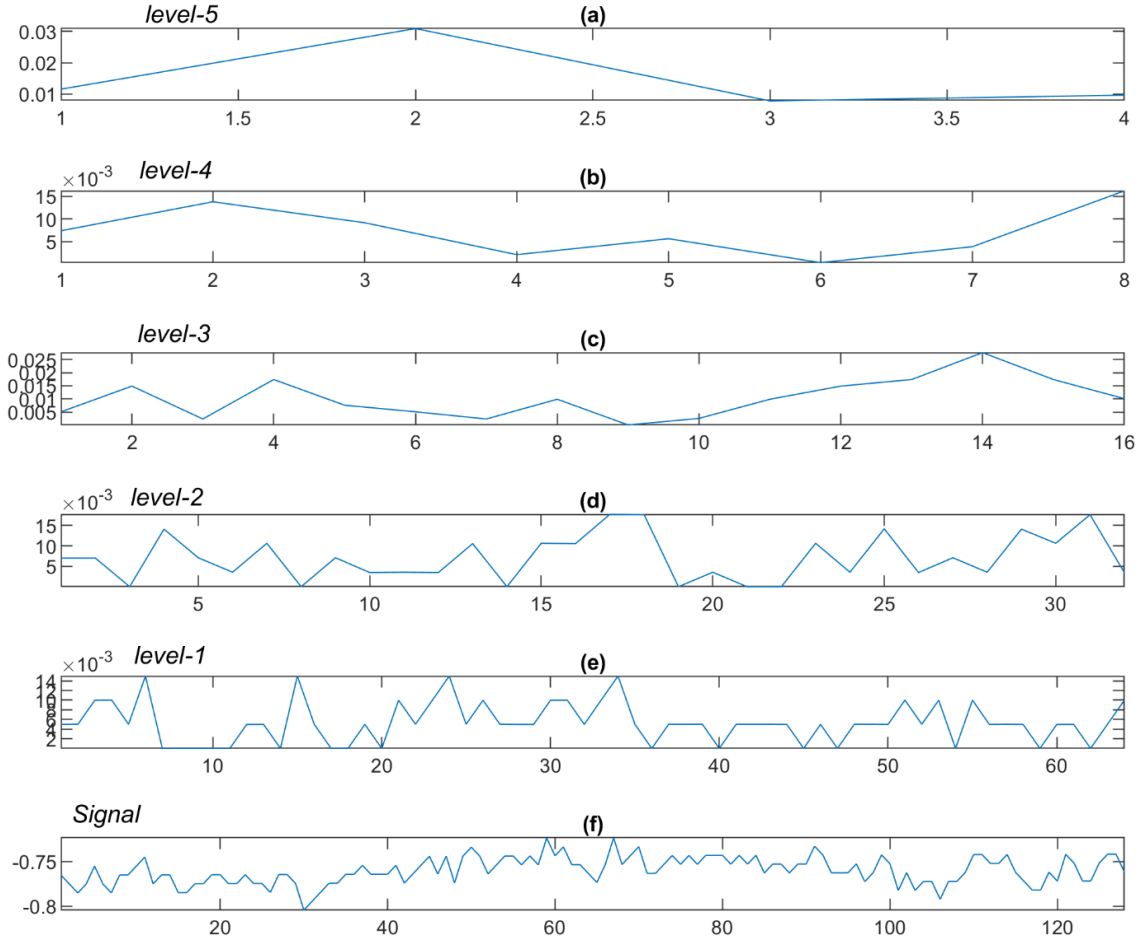

Figure 1. the test signal (f) and its decomposition at level 1 to 5 (e to a) using DWT transform.

(ii) The detail wavelet coefficient is used for computation of wavelet leaders (w_l) from each scale shown in Figure 2.

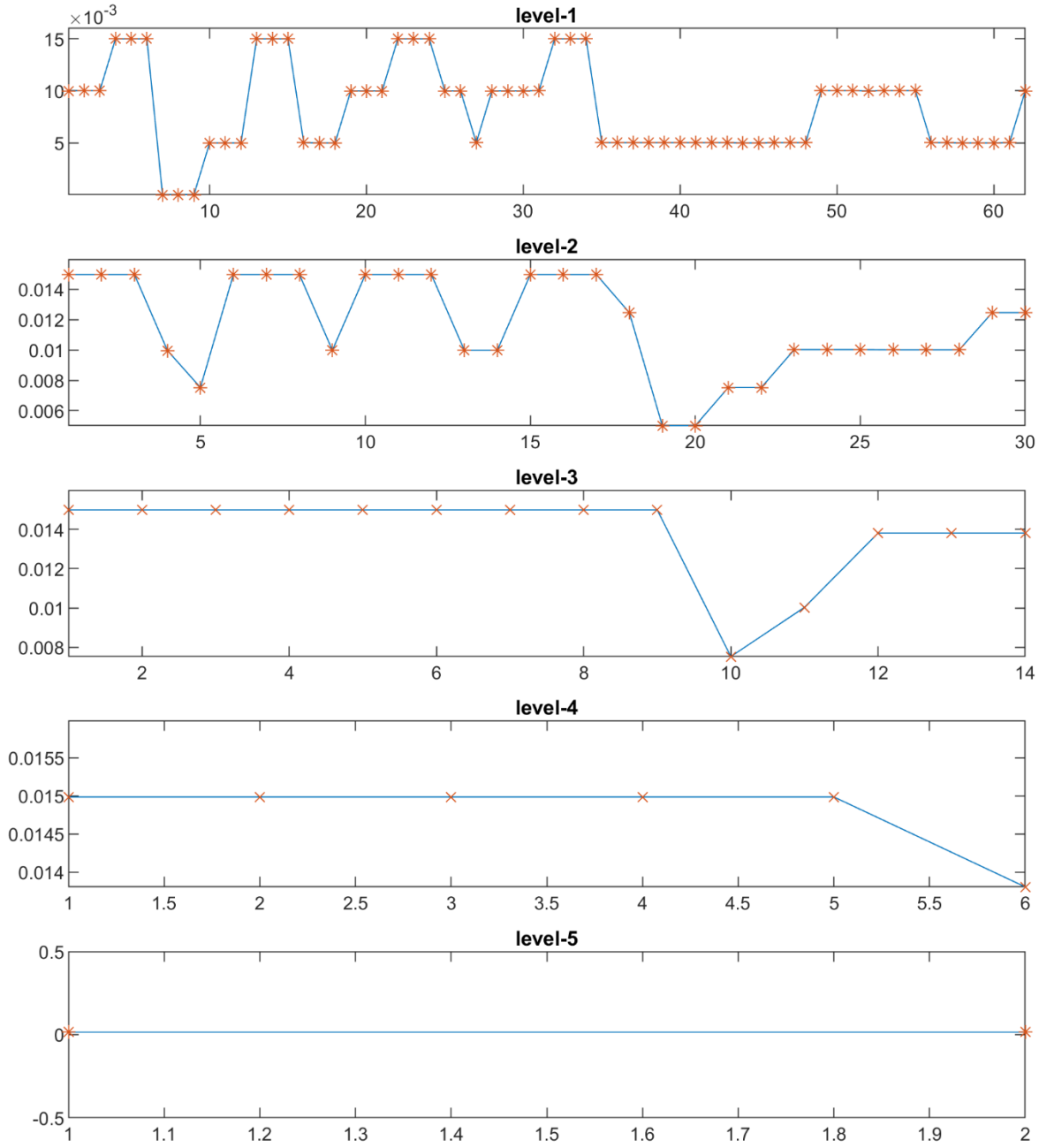

Figure 2. Wavelet leader selected from detail wavelet coefficients at level 1 to 5 (from top).

(iii) The w_l estimated at each scale is used to compute multiresolution structure function of multifractal parameter $\varphi_q, D_q, H_q,$ and C_p at linearly space moment order (q=-5 to +5), in which $D_q, and\ H_q$ are the parameters of the multifractal spectrum. The equations involved to compute these parameters are explained clearly by Jaffard et al. (2007) and Serano and Figliola (2009). The variation of $D_q, and\ H_q$ from scale 2 to 5 at moment order q is shown in Figure 3a and b respectively.

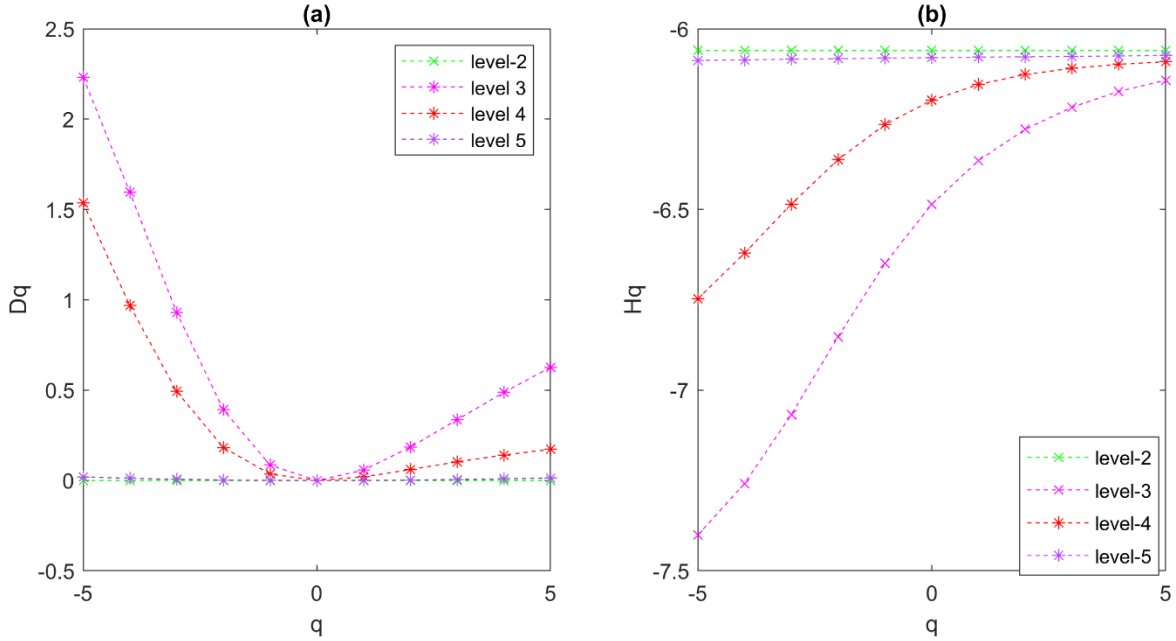

Figure 3. The variation in multifractal parameter (a) D_q and (b) H_q with moment order q at level 2 to 5.

(iv) At this stage, we have the values of multifractal parameters at scale one to five and moment order q. The final values of multifractal parameters correspond to q (-5 to +5) is the slope of linear regression of multifractal parameters measured at different scales verses log of scales. Thus, each value of multifractal parameters ($\varphi_q, D_q, H_{q,}$ and C_p) are now available with respect to moment order q(-5 to +5). The variation of $\varphi_q, D_q, and\ H_{q,}$ with respect to q is shown in Figure 4 a-c respectively, and multifractal spectrum ($H_{q,}$ vs D_q) shown in Figure 4d.

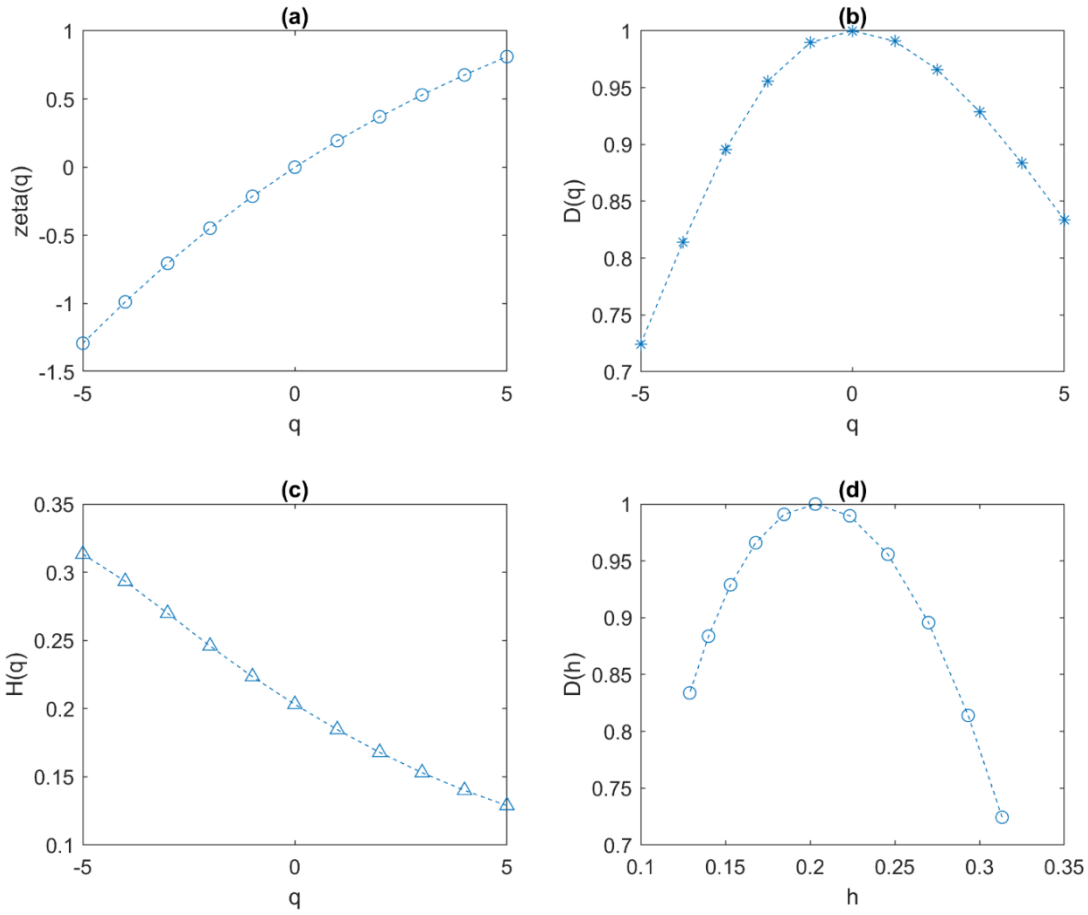

Figure 4. The variation in final multifractal parameters (a) φ , (b) D, (c) H with respect to moment order q and the spectrum of multifarctal parameter ($D\ vs.\ h$) is shown in (d).

To further establish the reliability of the computed multifractal spectrum values, we have tested this method on four different types of synthetic signals with known scaling exponents h1(0.2), h2(0.4), h3(0.6), and h4 (addition of h1, h2, and h3 in series). The small exponent indicates the less correlated or noisier signal, whereas signal of large exponent indicates high correlated or more smooth (Figure 5) data. For multifractal, the disturbed signals are expressed through higher degree of multifractal nature or large spectrum width than the spectrum width of less disturb or smooth signal i.e. spectrum width of h4>h1>h2>h3. Thus, we can say that the values are reliable and can fulfil the objective on application of geomagnetic data.

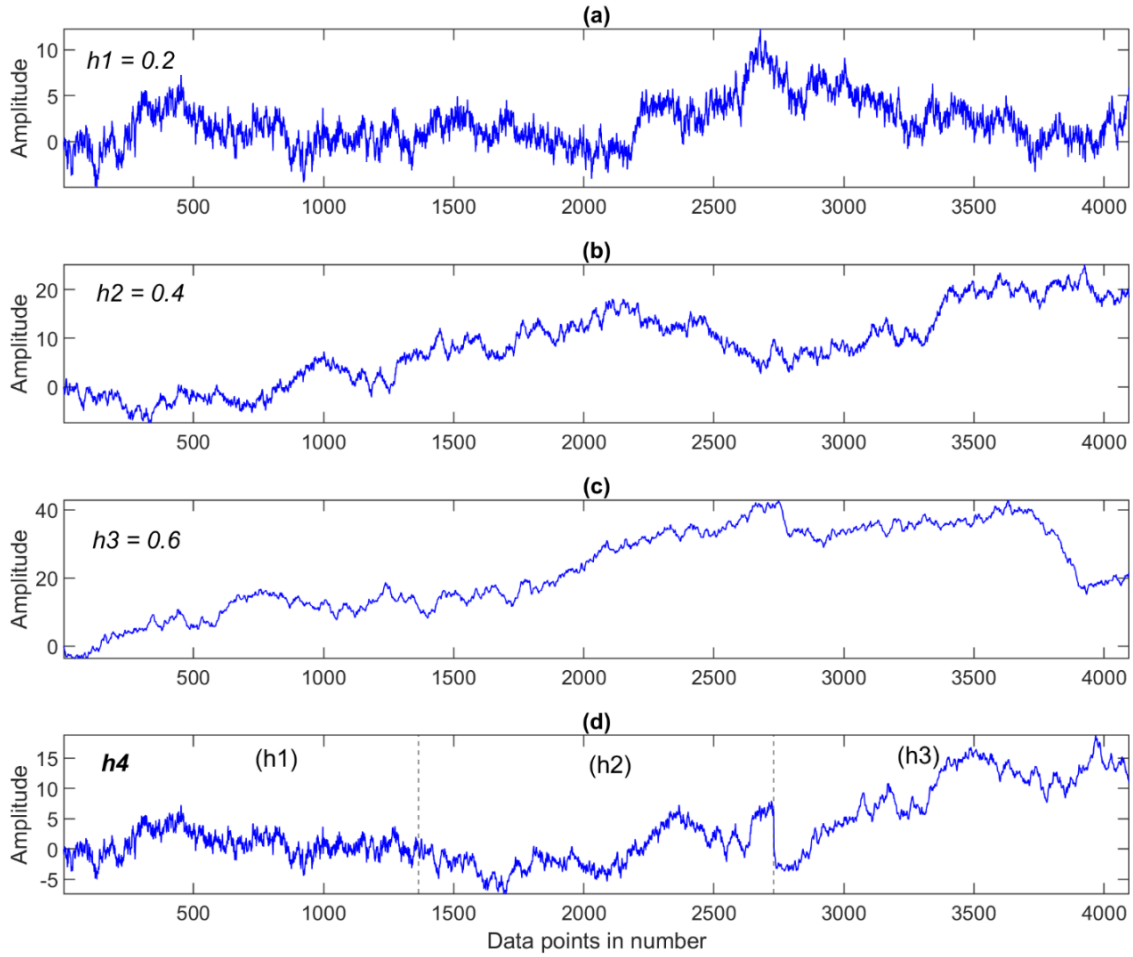

Figure 5. The synthetic signal generated at hurst exponent (a) 0.2, (b) 0.4, (c) 0.5, and (d) combination of all three in series.

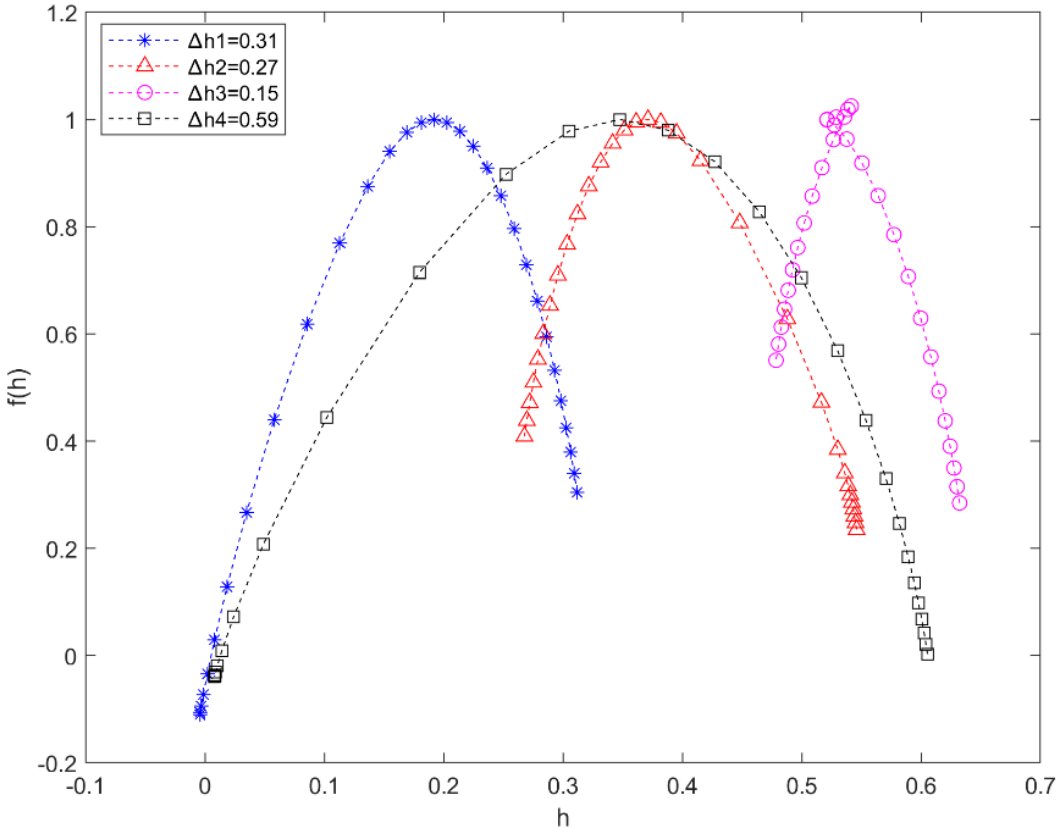

Figure 6. The multfarctal spctrum of signal h1, h2, h3, and h4 showing the degree of multifractality**.**

Comment 3. The English writing should be substantially re-written because there are many grammatical and typo errors. Meanwhile, the statements should be re-organized

Answer 3. We have improved English syntax throughout the manuscript.

Comment 4. In Table 1, the authors should replace 'Mod' and 'Large' for Mag (magnitude), 'Mod', 'Shallow', and 'Large' for 'Foc. D.' (Focal Depth),' and 'Mod', 'Small', ad 'Large' for 'Epi. D.' (Epicentral Distance)' by the magnitude range, focal depth range, and epicentral range in numbers.

Answer 4. Table 1 is revised and also the ranges of magnitude, focal depth, and epicentral distances listed in table caption. The revised table is incorporated at the end of this comment and answer section (Page 15).

Minor Problems

Comment 5. The abstract is not concise.

Answer 5. We have re-written the abstract. The revised abstract is reduced to 187 words from 202 words of original abstract as per norm of journal (100-200 words).

The revised abstract as follows:

"The emission of seismo-electromagnetic (EM) signatures prior to earthquake recorded in geomagnetic data has potential to reveal the pre-earthquake processes. This study focused to analysis of vertical component of a geomagnetic field from Mar 2019 to Apr 2020 using fractal and multifractal approach to identify the EM signatures in Campbell Bay, a seismically active region of Andaman and Nicobar. The significant enhancements in monofractal dimension and spectrum width components of multifractal highlights the complex nature of geomagnetic field due to interference of high frequency EM field, due to pre-earthquakes processes of micro fracturing of the shallow crust in the vicinity of the West Andaman Fault and Andaman Trench. On the other hand, the enhancements in holder exponents, highlight the complexities in the geomagnetic time series due to interference of less correlated, smooth, and low frequency EM field, suggesting that pre-earthquake processes on Seulimeum Strand (SS) are dominated by electrokinetic processes. The mono fractal, spectrum width, and holder exponent parameter reveals different nature of pre-earthquakes process prior to earthquakes with an average of 10, 12, and 20 days respectively, which are also lies in range of short -term earthquake prediction."

Comment 6. It is better to provide a figure to show an example of observed Z-component seismo-electromagnetic (EM) signatures.

Answer 6. To observe the EM signatures in vertical component of geomagnetic field in night time data (22:00-02:00), we have selected two quite days (25 May and 3 Aug, 2019) in which one (25th May) is interfered by EM field, while second (3 Aug) is not interfered by EM field. Figure 7a, b showing the field on and clearly deciphers the significant fluctuations in the field on 25th May, 2019 even on night time quite data, while field on 3rd Aug, 2019 does not showing such fluctuations on quite day. A significant enhancement in hw (Figure 7c) and hwp (Figure 7d) also marked on 25th May, 2019, while there in no such enhancements marked in hw and hwp on on 3rd Aug, 2019. This example of observation will be also included in manuscript.

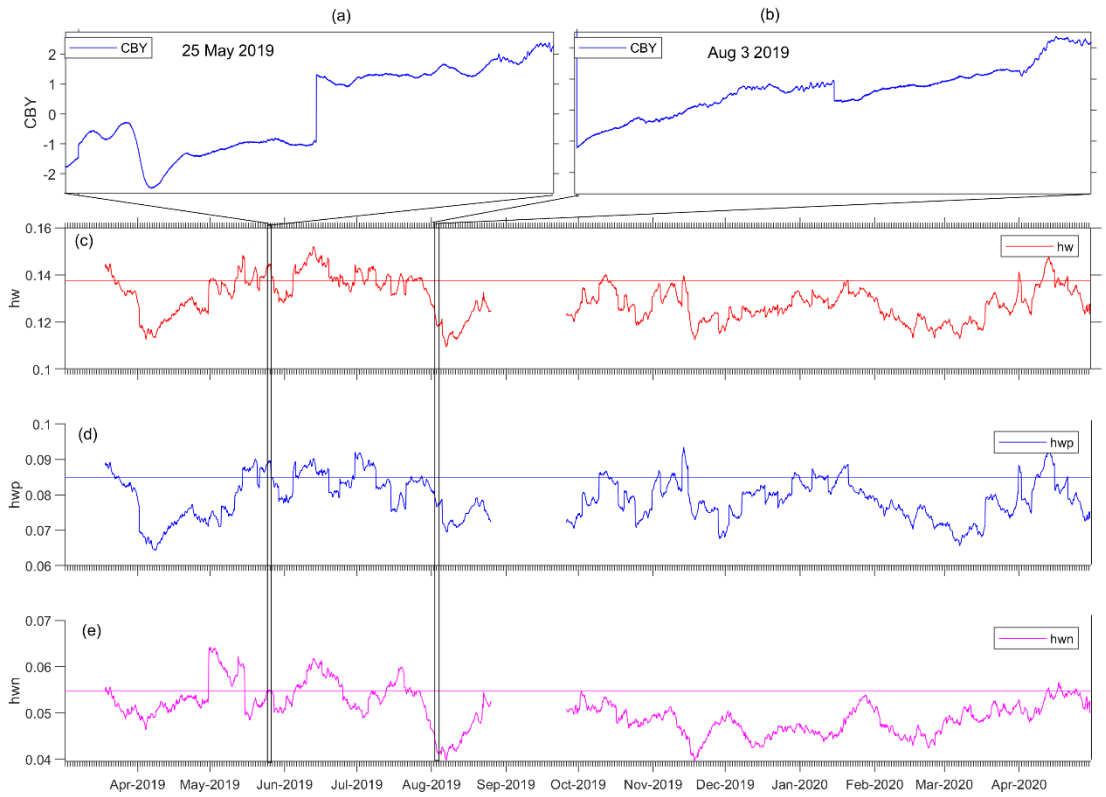

Figure 7. The night time data of vertical component of geomagnetic field on (a) 25th May, 2019 and (b) 3rd Aug, 2019. The multifractal component of (a) hw, (b) hwp, and (c) hwn from Mar, 2019 to April, 2020.

Comment 7. The quality of figures should be improved

Answer 7. All Figures in manuscript are 300 dpi. The resolution of Figure in manuscript will be enhanced by 600 dpi at the time of submission of revised manuscript.

Revised part methodology section:

2. Methodological Approach

It is proposed to apply both fractal and multifractal approaches to the Z component time series, to distinguish between the different source characteristics and examine their relationship to earthquake parameters. The Z-component of 1 Hz geomagnetic signal is preferred because it is more prone to be affected by the local EM field generated by lithospheric deformation.

Gotoh et al. (2003) tested different methods for estimation of fractal dimension of geomagnetic signal and suggested that the fractal dimension value using Higuchi method, is more reliable and consistent than others. In Higuchi method, a time series x(n) is decomposed into time series of different lengths x_k^m, defined as:

$$x_k^m : x(m), x(m+k), x(m+2k), \ldots\ldots x\left(m+\left(\frac{N-k}{k}\right).k\right),$$

Where, n is 1,2 ,3 …N, m is 1,2,3…k, and k is 1,…., k_{max}. The average length of decomposed time series $L_m(k)$ computed at interval of time from $k = 1$ to k_{max} are related to each other as:

$$L(k) \propto k^{-f_D}$$

Where L is average length of decomposed time series , f_D is fractal dimension equal to the slope of fitted line over $\log(L(k))$ versus $\log\left(1/k\right)$.

In our analysis, we have adopted the Higuchi method for monofractal analysis. Application of Higuchi method on night-time (22:00-02:00 LT) Z-component of geomagnetic signal of 3 April 2019, is shown in Figure 2 to verify the appropriateness of this approach.

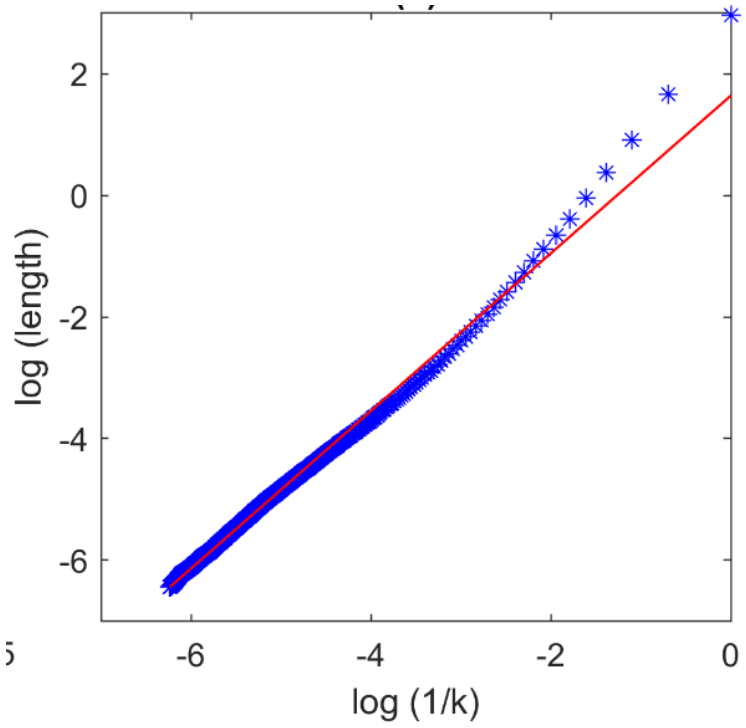

Figure 2. The linear fitting over log of average length and log of size of time interval (scale) showing the power law nature of geomagnetic signal.

Muzy et al. (1994) proposed an approach for multifractal analysis based on discrete wavelet or wavelet leader. In this approach, the local suprema $f_{i,k}$ is obtained from discrete wavelet coefficients at dyadic scales, where, k is translation parameter, i is scale, and the position in time for dyadic interval is $2^i k$ (Jaffard et al., 2006; Wendt et al., 2008). The local suprema of wavelet coefficients $f_{i,k}$ obtained at dyadic scale, aid in computation of the multiresolution structure function $S_{xL}(q,i)$ for to produce the global holder exponent (Serrano and Figliola, 2009) i.e.

$$S(q,i) \sim (2^i)^{\tau(q)}$$

Where, i is scale, q is moment and $\tau(q)$ is scaling exponent. The scaling exponent follows power law relation can be estimated by following relation

$$\tau(q) = \lim_{i \to 0} inf \frac{log(S_{xL}(q,i))}{log(2^i)}$$

The spectrum of global holder exponent is derived from multifractal formalism using legendre function (Serrano and Figliola, 2009), which leads to.

$$f(\alpha) = \inf(1 - \tau(q) + \alpha(q) * q),$$

Where α is global holder exponent and $f(\alpha)$ is function of global holder exponent. The degree of intermittency or multifractality is defined by multifractal or singularity spectrum i.e. $\Delta\,\alpha = \alpha_{max} - \alpha_{min}$. Larger the width of multifractal spectrum, larger is the multifractality or intermittency, and vice-versa. The width of multifractal spectrum h_w (from $-q\ to + q$) indicates the overall degree of multifractality of signal. The spectrum width h_{wp} ($q > 0$) and h_{wn} ($q < 0$) indicates the weaker and stronger singularity of multifractal signal. The h_{max}-h_{min} curve defines the average fluctuations embedded in the signal while $h(0)$ represents the zero-order exponent or monofractal dimension (Hayakawa et al., 1999). Similarly, f_{max} define the exponent which occurred maximum number of times. Application of multifractal on nighttime (22:00-02:00 LT) Z-component of geomagnetic signal of 3 April 2019, is shown in Figure 3. Thus the wavelet leader approach is adopted in this study due to contact support for wide range of q $(-q\ to + q)$ and stability for scaling function for negative q values compared to other techniques.

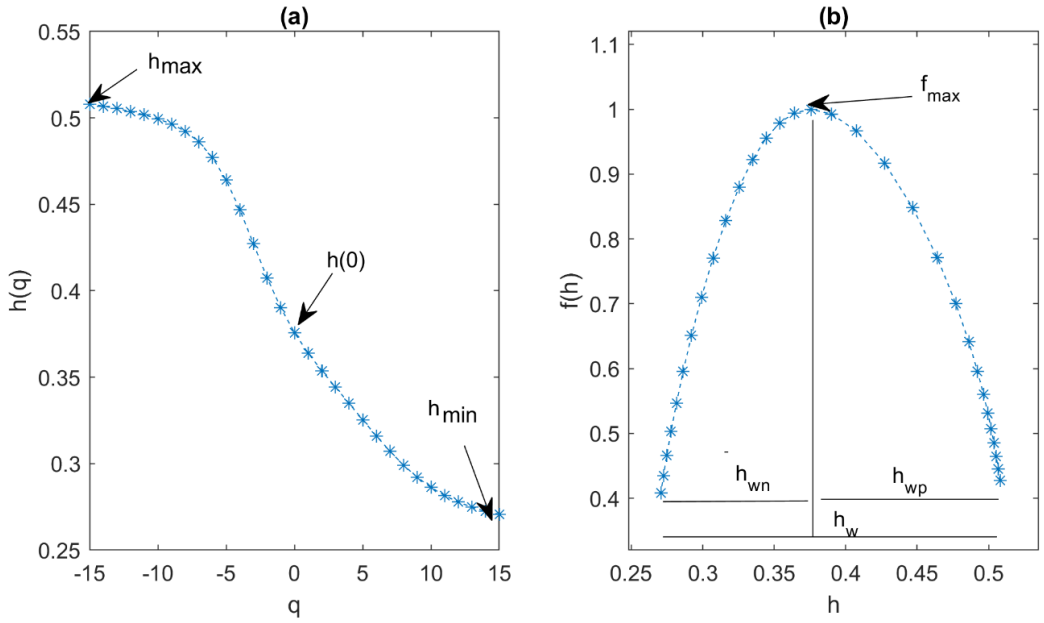

Figure 3. The multifractal analysis for 1800 samples of 3rd April 2019, where (a) The variation of holder exponent (h) with moment order q in range of -15 to +15 showing as h_{min}, h_{max}, and $h(0)$. (b) Multifractal spectrum showing the width of spectrum h_w, h_{wp} and h_{wn}.

From the same data, from fractal analysis, the power law behaviour, and from multifractal, the finite width of multifractal spectrum and variation in holder exponent demonstrates the fractal as well as multifractal natures of the signal.

The fractal dimension f_D of the total duration of Z-component data is calculated for consecutive time windows of 30 min to trace the variations of the fractal dimension, producing eight values for each day. The choice of a 30 min time window (consisting of 1800 data points) is based on the balance between the stability of fluctuations in fractal dimension and minimizing loss of information after trials with 15 min and 1 hr. time windows.

Similarly, the spectrum width parameter ($h_w, h_{wp}, and\ h_{wn}$) and holder exponent parameter h_{max}, h_{min} and, $h(0)$ estimated for the total length of Z component from window of 30 minute to identify the degree of singularity or complexity (global, weaker, and stronger) as well as degree of fluctuations with respect to amplitude (from smaller to larger). The shorter fluctuations in fractal dimensions are smoothed by applying a 15-day moving mean.

The increments in fractal dimension and multifractal parameter (spectrum width and holder exponent) value greater than the threshold value ($\mu + \sigma$) are considered as a significant evidence of existence of EM signals of lithospheric origin.

Table 1: The following table summarizes the earthquake and its characteristics presence (Y) or absence (-) of potential enhancements in monofractal (f_D) and multifractal (h_w, f_{max}, h_{max}) components and diurnal ratio. The characteristics of earthquakes are given by it range of Magnitude (moderate: 4.5≤M<5, large: M≥5.0), focal depth (shallow: f≤25km, moderate: 25≤f<80km, large: f≥80km), and epicentral distance (small: ed≤60km, moderate: 60<ed≤150, large: ed>150).

EQ. No.	Magnitude	Focal Depth (Km)	Epicentral Distance (Km)	Single/ Cluster	f_D	h_w	f_{max}	h_{max}	Diurnal ratio
1-45	Moderate to Large	Moderate	Moderate	C	-	Y	Co-	-	-
46-48	Moderate	Moderate	Moderate	C	-	-	Y	Y	Y
49	Moderate	Moderate	Moderate	S	Co-	Y	-	-	Y
50-51	Moderate	large/ shallow	Large	C	Y	Y	-	-	Post-
52	Moderate	Shallow	Large	S	-	-	-	-	Y
53-54-55	Moderate to Large	Shallow	Small to Moderate	C	Y	Y	Y	Y	Y
56	Moderate	Moderate	Large	S	Y	-	-	-	-
57	Large	Shallow	Large	S	Y	-	-	-	-
58	Large	Large	Moderate	S	Y	-	-	-	-
59	Moderate	Shallow	Large	S	-	-	-	-	Y
60	Moderate	Large	Moderate	S	Co-	-	-	-	Y
61	Moderate	Shallow	Large	S	Co-	-	-	-	Y
62	Moderate	Shallow	Large	S	-	-	-	-	-
63	Moderate	Shallow	Large	S	-	-	-	-	post